NCTAM 2012

9th National Congress on Theoretical and Applied Mechanics

Ecole Royale Militaire
Avenue de la Renaissance 30
B-1000 Bruxelles

www.rma.ac.be

Koninklijke Militaire School
Renaissancelaan 30
B-1000 Brussel

CONFERENCE PROCEEDINGS

9-10 May 2012

ROYAL MILITARY ACADEMY

ISBN 978-2-8052-0151-6

Ed. Walter BOSSCHAERTS
Bart JANSSENS
Benoît MARINUS

.be

nctam@rma.ac.be
http://meca.rma.ac.be/nctam

NCTAM 2012 conference proceedings

Manufacturing and Machine design 2

- Bionic Assembly System: Hybrid Control Structure, Working Scenario And Scheduling
- Regression Rate Study In A Small Hybrid Rocket Engine Using N2O/Paraffin Propellant
- Design For Machining - Optimizing The Turning Operation

Mechatronics 1

- Multi-Robot Coordination In Transport Mission
- Study Of The Propulsion System Of A Vtol Muav Using Fuel Cells
- Simulation Framework Of Modular Robots Using Easydyn
- A System Analysis Approach In Safe Machine Design For Nuclear Applications: Myrrha In-Vessel Fuel Manipulation
- Predictive Cruise Control For Dual Driven Electric Vehicles Based On Trajectory And Aerodynamics

Mechatronics 2

- Experimental Comparison Of Kinematics And Control Interfaces For Laparoscope Positioners
- Electronic Hardware Architecture Of Step Rehabilitation Robot Altacro
- Overview Of A Test-Setup To Research Software And Hardware Innovations On The Way To Safe Human Robot Interaction
- About The Design Of The Social Robot Probo, Facilitator For Asd Therapies
- Pneumatic Tactile Display Controlled By A Miniaturised Proportional Valve

Structural Mechanics 1

- Finite-Element Analysis Of The Static/Dynamic Mechanical Reliability Of Adhesively Bonded Electronic Components.
- Robust Topology Optimization Accounting For Misplacement Of Material
- Efficient Prescription Of Mortars For Durable Masonry Restorations: Experimental Study Comparing The Mar With Granular-Based Calculations.

Structural Mechanics 2

- Determination Of Axial Forces By Local Vibration Measurements
- Optimal Design Of Shells With Fe Based Parameterization
- Bi-Potential And Meshless Methods: Towards New Challenges In Soil Mechanics.
- Detecting And Quantifying The Impact Of Soil Defects In Masonry Systems: Challenges And Recourse To A Distributed Network Analysis Method
- Out-Of-Plane Behaviour Of Urm Walls: Experimental Studies

Theoretical Mechanics

- Study Of The Resistance Of Bollards Against Impact Loads
- An Invariant Representation To Facilitate Recognition Of Rigid Body Motion Trajectories

Vibrations 1

- An Efficient Experimental/Finite-Element Approach For Modal Identification Of A Fastened Unattainable Space Electronic Module
- Numerical Modeling Of Seismic Wave Propagation: Towards Stable Perfectly Matched Layers For Time Domain Elastodynamics
- Localized Force Identification And Response Prediction On A Footbridge
- Numerical Simulation Of Long And Slender Cylinders Vibrating In Axial Flow Applied To The Myrrha Reactor
- Random Vibration Testing Using A Pseudo-Random Method With Crest-Factor Limiting: An Experimental Comparison With The Classical Method

Vibrations 2

- Experimental And Numerical Determination Of Transfer Functions Along Railway Tracks
- Combined Experimental-Numerical Characterisation Of The Vibro-Acoustic Properties Of Lightweight Panels

Vibrations 3

- Prediction Of Ground Vibration Generated By A Multi-Head Pavement Breaker
- A Numerical Study Of Subgrade Stiffening As A Mitigation Measure For Railway Induced Vibrations
- A Wave Based Model To Predict The Sound Transmission Through Multilayered Structures Between Two Rooms

Numerical simulation of long and slender cylinders vibrating in axial flow applied to the MYRRHA reactor

J. De Ridder [1], J. Degroote [1], K. Van Tichelen [2], J. Vierendeels [1]
[1]Universiteit Gent, Department of Flow, Heat and Combustion Mechanics
Sint-Pietersnieuwstraat 41, 9000 Gent, Belgium
[2]SCK•CEN
Belgian Nuclear Research Center, Boeretang 200, 2400 Mol
email: j.deridder@ugent.be, joris.degroote@ugent.be, jan.vierendeels@ugent.be,kvtichel@SCKCEN.be

Abstract— **Flow induced vibrations are an important concern in the design of nuclear reactors. One of the possible designs of the 4^{th} generation nuclear reactors is a lead-cooled fast reactor of which MYYRHA is a prototype. The combination of high liquid density, flow velocity, low pitch-to-diameter ratio and the absence of grid spacers makes this design prone to flow induced vibrations. Although most vibrations are induced by cross flow, axial flow around this slender structure could also induce vibrations.**
In order to gain insight in the possible vibrations (either induced by cross flow, axial flow or an external excitation) this study examines the change of eigenmodes and frequencies of a bare rod due to the lead-bismuth flow. To do so partitioned simulations of the fluid structure interaction are performed in which the structure is initially perturbed according to an in-air eigenmode.

Keywords— **Flow induced vibrations, partitioned numerical simulation, eigenmodes, axial flow**

I. Introduction

FLOW induced vibrations are an important concern in the design of heat exchangers and nuclear reactors. Most of the times flow induced vibrations arise from cross flow [1]. However, even axial flow could give rise to vibrations, e.g. in nuclear reactors [2]. Typically the occurrence of flow induced vibrations increases with higher flow velocities, higher fluid density and in the case of tube bundles with lower pitch-to-diameter ratios.

These conditions are likely to be met in the MYRRHA-reactor, which is currently being developed as a prototype nuclear reactor of the 4^{th} generation [3]. It is a fast reactor with lead-bismuth as coolant. The main advantage of this type of reactor is the improved usage of the nuclear fuel, which leads to less nuclear waste and waste with a shorter lifetime. Additionally it can have a higher conversion of nuclear waste due to the possibility of transmutation. To ensure a low pressure drop, wire wrapped fuel rods will be used instead of classical grid spacers. The combination of these operating conditions could give rise to unwanted vibrations of these rods.

Currently, effective mass and damping of these structures immersed in fluid are mostly determined from semi-empirical formulas or force coefficients obtained from 2-dimensional computational fluid dynamics [5]. In this paper a time-domain method will be proposed, which results in vibration characteristics, while solving the 3-dimensional Navier-Stokes equations.

II. Methodology

The aim of numerical experiments is to obtain eigenfrequencies, mode shapes and damping ratios of the structure in contact with the fluid, while solving the Navier-Stokes equations and thus taking all non-linearities in the flow field into account. To obtain information of an eigenmode in fluid, the undeformed structure exposed to the fluid flow is perturbed according to the corresponding eigenmode in-vacuo.

Initially an in-vacuo eigenmode analysis of the structure is performed using Abaqus, a finite element solver. The resulting mode shapes will be used as initial condition in time-domain fluid-structure simulations.

In order to avoid overlap of the fluid domain and the solid domain, the first part in the FSI-simulation is a steady-state calculation with the undeformed structure. In the second part the structure is deformed according to the mode shape, coming from the in vacuo eigenmode analysis. The fluid mesh is deformed accordingly and a steady-state flow is calculated around the rigid, deformed structure. In the final part, the structure is allowed to move and the resulting vibration is calculated using an unsteady FSI-simulation.

The fluid-structure interaction (FSI) itself is calculated in a partitioned way using the IQN-LS algorithm [6], with Fluent as flow solver and Abaqus as structural solver. The interface quasi-Newton with on approximation of the Jacobian based an a least squares solution algorithm belongs to the strongly coupled algorithms, meaning that both the kinematic and the dynamic condition on the fluid-structure interface are satisfied in each time step. Gauss-Seidel iterations between the flow and the structural solver do not converge, so the IQN-LS algorithm is used instead.

The resulting vibration can be characterized by fitting a

function to the resulting displacement.

$$y_{disp} = \sum_i A_i \exp(-c_i t)\sin(\omega_i t + \phi_i) \quad (1)$$

As the eigenmodes in the Pb-Bi are not necessarily equal to those in vacuo, it was necessary to fit lower eigenmodes than the initially imposed eigenmode as well. To determine for example the characteristics of the fourth eigenmode, the amplitude and phase of the previous three eigenmodes are also fitted.

III. Case definition

In this paper a reduced model of the fuel rod bundle has been used. Only one rod is considered instead of an entire rod bundle. As the aim of this paper is to see the influence of the Pb-Bi flow on a rod-like structure, the rod is replaced by a steel hollow circular cylinder (Young's elasticity modulus $E = 200GPa$, Poisson ratio $\nu = 0.30$, solid density $\rho_s = 7800kg/m^3$), with a length of 1.5m.

This rod-like structure is placed in a hexagonal cylinder, which forms a periodic unit of the rod bundle, see Figure 1. At the boundaries of the hexagonal cylinder, parallel to the rod wall, a symmetry condition for the fluid flow is imposed. At the inlet, which is located at the bottom (z=0 m) of the simulation domain a velocity of 1.5 m/s is imposed. The outlet (at the top of the computational domain) is assumed to be at a fixed pressure.

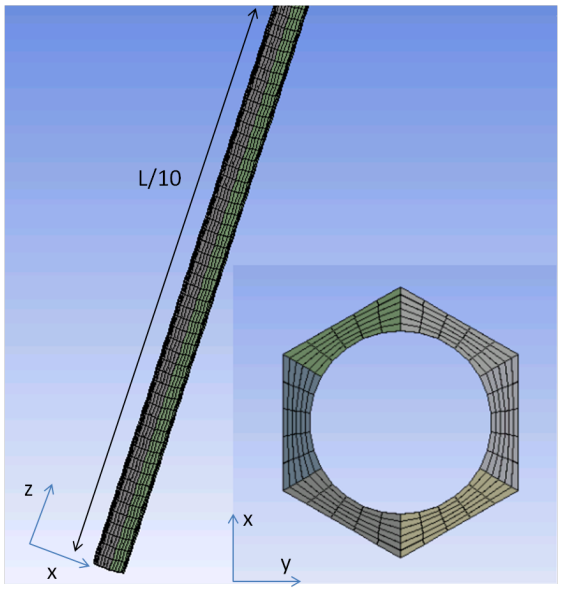

Fig. 1. Fluid domain mesh, projected along y-axis (left) and z-axis (right) .

The Pb-Bi flow (fluid density $\rho_f = 10300kg/m^3$, dynamic viscosity $\mu = 0.0017kgm/s$), with $Re \approx 50000$ is turbulent. To account for the turbulence the k-ω SST model is used. At the inlet a turbulent intensity of 10% and a turbulent length scale of 1 mm are applied.

IV. Results and discussion

A. Convergence

The grid convergence of the fluid grid is tested by refinements in three directions: radial, circumferential and axial. The different computational meshes are used to calculate the behaviour of the second eigenmode of a single tube in a symmetrically confined flow. Originally, the grid convergence study was performed with the first eigenmode. The first eigenmode is however heavily damped with respect to the number of timesteps, so the second eigenmode is used instead, as a more stringent test.

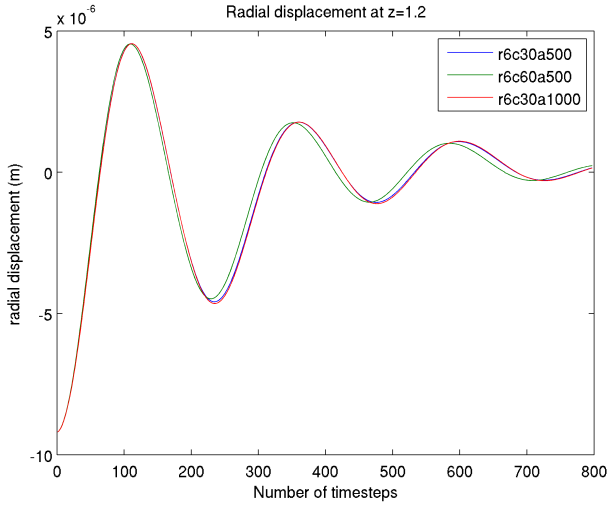

Fig. 2. Effect of circumferential and axial refinement on second mode vibration. The legend denotes the number of radial, circumferential and axial divisions.

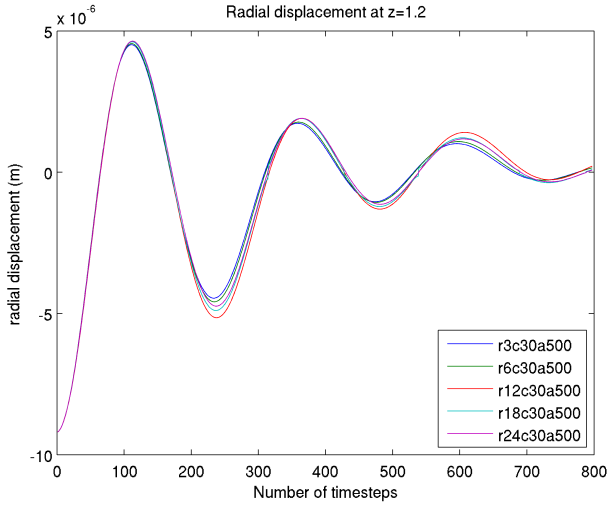

Fig. 3. Effect of radial refinement on second mode vibration. The legend denotes the number of radial, circumferential and axial divisions.

The results of this grid convergence study is shown in Figures 2,3. The curves are labeled with the number of radial divisions (r), circumferential divisions around the cylinder (c) and axial divisions (a) of the fluid mesh. A typical mesh used is depicted in Figure 1. From Figure 2 the mesh refinement in the circumferential and axial direction are barely influencing the resulting vibration, apart from a small change in frequency for the circumferential refinement.

In the radial direction four different meshes are constructed, with respectively 3,6,12,18 and 24 radial divisions. The first two mesh results in y^+-values: 40 - 70, meaning that the first grid point is in the logarithmic sublayer, while the other meshes have y^+-values: 1-2.5 and have their first grid point in the viscous sublayer. To achieve this, different growth rates are applied. The accuracy of the solution is however not very dependent on whether the first grid point is in the logarithmic or the viscous sublayer, but on the regularity of the grid. From Figure 3 the displacements of the viscous sublayer meshes are evolving towards the solution with the logarithmic sublayer mesh.

The influence of time step size on the characteristic vibration of the first four eigenmodes shows that frequencies are almost insensitive to time step size, while damping typically is more dependent on time step size. The data in Table I are obtained at a point with z=1.2m. The influence of time step with respect to damping is considered to be converged when approximately 200 time steps per period are used. This relatively high number of time steps results from the first-order time accuracy of the used scheme.

TABLE I
VIBRATION CHARACTERISTICS FOR THE FIRST TWO EIGENMODES WITH DIFFERENT TIME STEP SIZES.

$\Delta t(ms)$	$f_1(Hz)$	$c_1(s^{-1})$	$\Delta t(ms)$	$f_2(Hz)$	$c_2(s^{-1})$
5	2.20	6.66	1	8.19	8.81
1	2.25	6.58	0.5	8.25	8.08
–	–	–	0.25	8.26	7.76

B. *Change of mode shapes*

Due to the interaction with the fluidum the bare notion of an eigenmode may no longer exist for the structure [7]. However, from the numerical simulations, a mode shape can be constructed. This mode shape is defined as the $A_i(z)$ in Equation 1, which are obtained by fitting Equation 1 to the radial displacements at every height.

The first mode shape is very similar in vacuo (determined from an eigenmode analysis) compared to the fitted mode shape in the Pb-Bi flow, see Figure 4. The two mode shapes are however not completely coinciding. The mode in the Pb-Bi flow is slightly shifted downstream. Note however that the downstream shift is very small ($5mm$) compared to the length of the tube ($1.5m$).

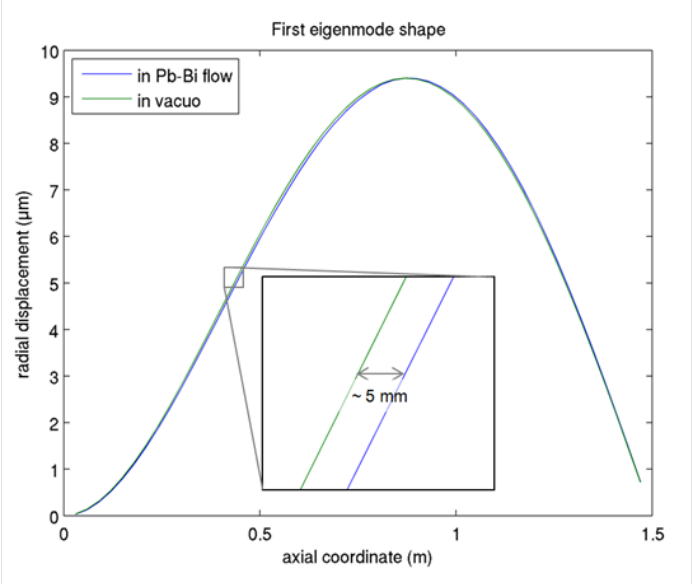

Fig. 4. First mode shape in vacuo and in Pb-Bi flow

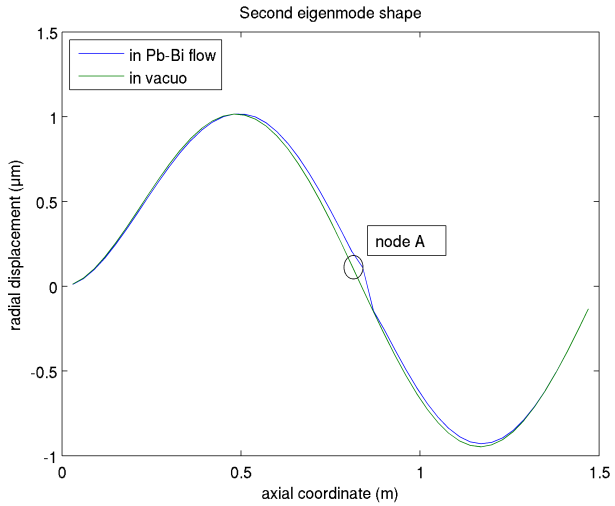

Fig. 5. Second mode shape in vacuo and in Pb-Bi flow

The fitting of the second mode shape in Pb-Bi flow provides only a rough estimate of the second mode shape in the vicinity of the node A, see Figure 5. At that point the resulting vibration comes from participation of the first mode. However, from Figure 5 , it becomes clear that the second mode shape is also very similar in vacuo or in the Pb-Bi flow.

TABLE II
VIBRATION CHARACTERISTICS FOR THE FIRST THREE MODES, FITTED AT Z = 1.2 M

	$f_1(Hz)$	$c_1(s^{-1})$	$f_2(Hz)$	$c_2(s^{-1})$	$f_3(Hz)$	$c_3(s^{-1})$
in vacuo	11.9	–	38.7	–	80.6	–
in turbulent Pb-Bi flow (k-ω SST)	2.20	6.66	8.25	8.08	17.5	10.32
in laminar Pb-Bi flow	2.5	1.9	8.4	2.6	17.6	3.9

C. *Resulting vibration characteristics*

The vibration characteristics of the first three eigenmodes, measured at z = 1.2m are listed in Table II. Note that c corresponds to the symbol used in Equation 1 and is the product of modal damping and the angular frequency.

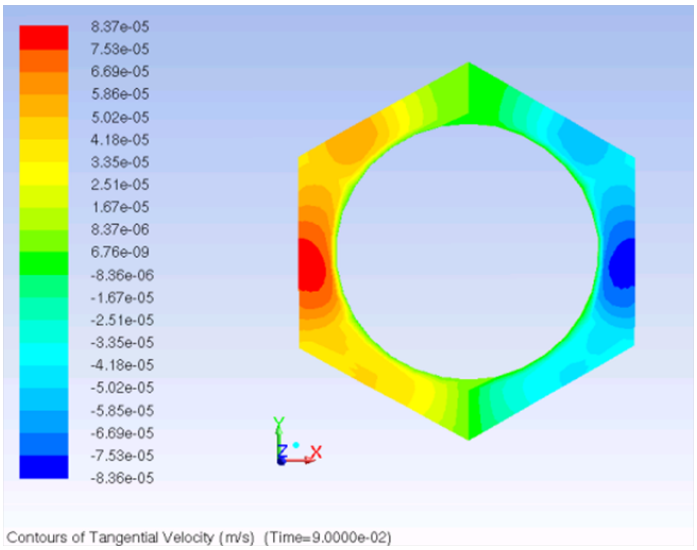

Fig. 6. Flow pattern around oscillating cylinder

The frequency of the tube vibration in Pb-Bi flow is much lower compared to the frequency of an in vacuo vibration, see Table II. This decrease in frequency can be explained by the added mass effect, which means that as the cylinder accelerates, the fluid around the cylinder also has to accelerate [8]. Intuitively it can be understood that a higher mass leads to a lower frequency, using $\omega^2 = k/m$, with k the stiffness and m the mass

Similarly a steadily moving cylinder will experience damping due to the fluid flow, as the fluid has to move (in the opposite direction of the cylinder motion), see Figure 6.

In Table II the results of a laminar calculation are also included. The vibration in the laminar flow is less damped than in the corresponding turbulent flow. In the turbulence model the effect of turbulence is included using a turbulent viscosity. As a result there will be more damping in the turbulent scenario. The turbulence in channel-like flow is however not isotropic, so where the laminar calculation may lead to an underestimation of the damping, the turbulent calculation may lead to an overestimation of the damping.

V. CONCLUSIONS

A numerical method which allows the determination of typical vibration characteristics in a fluid has been presented, while taking all non-linearities in the flow field into account. This numerical method had been applied to a flexible cylinder, vibrating in Pb-Bi flow.

The resulting mode shapes were similar for the vibration of the structure in vacuo or in Pb-Bi flow, although they were slightly shifted downsteam. The resulting frequency decreased significantly as a result of the added mass. Due to (turbulent) viscosity the motion was significantly damped.

ACKNOWLEDGMENTS

Jeroen De Ridder gratefully acknowledges a Ph.D. fellowship of the Research Foundation - Flanders (FWO).

REFERENCES

[1] M.J. Pettigrew, C.E. Taylor: Vibration analysis of shell-and-tube heat exchangers: an overview-Part 1: flow, damping, fluidelastic instability. *Journal of Fluids and Structures*, 18 (2003), 469-483.

[2] L. Wang, Q. Ni: Vibration of Slender Structures Subjected to Axial Flow or Axially Towed in Quiescent Flow. *Advances in Acoustics and Vibration*, 2009 (2009), Article ID 432340.

[3] H.A. Abderrahim, P. Baeten, D. De Bruyn, J. Heyse, P. Schuurmans, J. Wagemans: MYRRHA, a Multipurpose hYbrid Research Reactor for High-end Applications. *Nuclear Physics News*, 20 (2010), 24–28.

[4] M.K. Au-Yang: Flow-Induced Vibration of Power and Process Plant Components. Professional Engineering Publishing, 2001.

[5] M. Hassan, A. Gerber, H. Omar: Numerical Estimation of Fluidelastic Instability in Tube Arrays. *Journal of Pressure Vessel Technology-Transactions of the Asme*, 132 (2010), 041307-1:11.

[6] J. Degroote, K.-J. Bathe, J. Vierendeels: Performance of a new partitioned procedure versus a monolithic procedure in fluid-structure interaction. *Computers & Structures*, 87 (2009), 793-801.

[7] M.P. Paidoussis: Fluid-Structure Interaction: Slender Structures and Axial Flow, Vol. 1. Academic Press, 1998.

[8] M.P. Paidoussis: Fluid-Structure Interaction: Slender Structures and Axial Flow, Vol. 2. Elsevier Academic Press, 2004.